

## First-principles calculations of metal stabilized Si<sub>20</sub> cages

Q. Sun, Q. Wang, T. M. Briere, V. Kumar, and Y. Kawazoe  
*Institute for Materials Research, Tohoku University, Sendai 980-77, Japan*

P. Jena

*Physics Department, Virginia Commonwealth University, Richmond, Virginia 23284-2000*

(Received 4 March 2002; published 31 May 2002)

It is well known that  $sp^2$  bonding in carbon can result in stable cage structures, but pure Si clusters with similar cage structures are unstable. Using first-principles calculations, we show that a dodecahedral cage of silicon can be stabilized dynamically as well as energetically by doping with Ba, Sr, Ca, Zr, and Pb atoms to create structures of silicon similar to that of the smallest carbon fullerene. The stability and bonding in such cages shed light on Si clathrates in which Si<sub>20</sub> is the basic building block of the structure. Moreover, the charge distributions and highest-occupied–lowest-unoccupied molecular orbital gaps for these cage structures can be tuned by changing the metal atom. This allows additional freedom for the design of nanomaterials involving Si.

DOI: 10.1103/PhysRevB.65.235417

PACS number(s): 73.22.-f, 36.40.Cg, 61.46.+w, 71.15.Nc

Carbon and silicon are members of the same group in the periodic table, though their chemical behaviors are quite different. Carbon atoms can form single, double, and triple bonds with themselves and other atoms that allow exhibition of very rich structures—graphite, diamond, fullerenes, nanotubes, amorphous structures, porous structures, graphite intercalated compounds (GIC's), and so on. These carbon-based materials display novel properties ranging from insulating to superconducting. However, the larger number of core electrons in Si makes it much more difficult for two Si atoms to form double or triple bonds. Consequently, Si prefers to form multidirectional single bonds ( $sp^3$ ). Although silicon has great potential applications in computer chips, microelectronic devices, catalysis, and new superconducting compounds, the possibility of using Si clusters in nanodevices has not yet attracted the same attention as carbon-based nanostructures have. This is primarily due to the discovery of C<sub>60</sub> (Ref. 1) and carbon nanotubes.<sup>2</sup> In turn, though, the rich structures and novel properties of fullerenes and carbon nanotubes have excited the imaginations of scientists over the world who have raced to find ways of making silicon similar to carbon.

Recently, doping of transition-metal atoms has been used to prepare caged clusters of silicon. In one such effort, large abundances have been reported for W@Si<sub>12</sub>, which has a metal-encapsulated hexagonal prism structure.<sup>3</sup> Kumar and Kawazoe<sup>4</sup> have performed first-principles computer simulations and predicted fullerene-like cage  $M@Si_{16}$  ( $M = \text{Hf}$  and  $\text{Zr}$ ), Frank-Kasper polyhedral  $M@Si_{16}$  ( $M = \text{Ti}$  and  $\text{Hf}$ ), and cubic  $M@Si_{14}$  ( $M = \text{Fe}$ ,  $\text{Ru}$ , and  $\text{Os}$ ) as well as 15- and 16-silicon-atom cage clusters encapsulating Cr, Mo, and W atoms. These silicon cage clusters are attractive for device applications due to the wide range of possible band gaps and because the presently available manufacturing processes are designed to produce silicon components.

These intriguing results for Si-based clusters leave some open questions that demand further exploration. For example, compared with carbon cage clusters, these doped Si clusters are smaller in size and in most cases the structures themselves are quite different from the fullerenes. Is it pos-

sible to create stable Si clusters with the smallest fullerene cage structure? We know that the smallest fullerene cage is C<sub>20</sub>, which has a dodecahedral structure.<sup>5,6</sup> How about the Si<sub>20</sub> cluster? Many studies have been devoted to pure Si clusters, and it has been well established that the ground state of Si<sub>20</sub> has a prolate-type structure with stacking of Si<sub>10</sub> tetra-capped trigonal prisms units.<sup>7–11</sup> However, the Si<sub>20</sub> cage is the basic building block for Si-clathrate materials, such as Ba<sub>6</sub>Ce<sub>2</sub>Au<sub>4</sub>Si<sub>42</sub>,<sup>12</sup> Si<sub>34</sub>,<sup>13</sup> Si<sub>46</sub>,<sup>14</sup> Ba<sub>24</sub>Si<sub>100</sub>,<sup>15</sup> and Si<sub>136</sub>.<sup>16</sup> Is it possible to maintain a stable cage structure for isolated Si<sub>20</sub>? This is important not only for Si-based nanodevices but also for understanding the stability of Si clathrates. In this paper, we use first-principles calculations to try to design new structures for Si that behave more like cousins and not just neighbors of carbon.

We use a linear combination of atomic orbitals centered at each atomic site for the cluster wave function and hybrid density functional theory to describe the exchange-correlation energies. The calculations are performed using the gaussian 98 package<sup>17</sup> at the B3LYP level of theory<sup>18</sup> with the LanL2DZ effective core potential basis set.<sup>19,20</sup> The applicability of the basis set and exchange correlation functional is verified from calculations of the ionization potentials (IP's) of various atoms,<sup>21</sup> which are in good agreement with the experimental values.<sup>22</sup>

As the stability of the geometrical structure is a key issue and *conventional* geometry optimizations generally converge to a structure in either a local minimum of the potential energy surface or a saddle point, dynamical stability analysis becomes an important tool. In the case of a saddle point, the system displays one or more imaginary vibrational frequencies, suggesting that the energy of the system can be lowered by structural displacements. In our calculations, the intrinsic stability of the structure is verified by calculation of the vibrational frequencies. The atomic positions are relaxed without symmetry constraint and the optimization is terminated when all the forces acting on the ions become less than 0.001 eV/Å.

We considered several possibilities to stabilize the Si<sub>20</sub> cage: (1) Following the analogy of stabilizing Si<sub>60</sub> by encap-

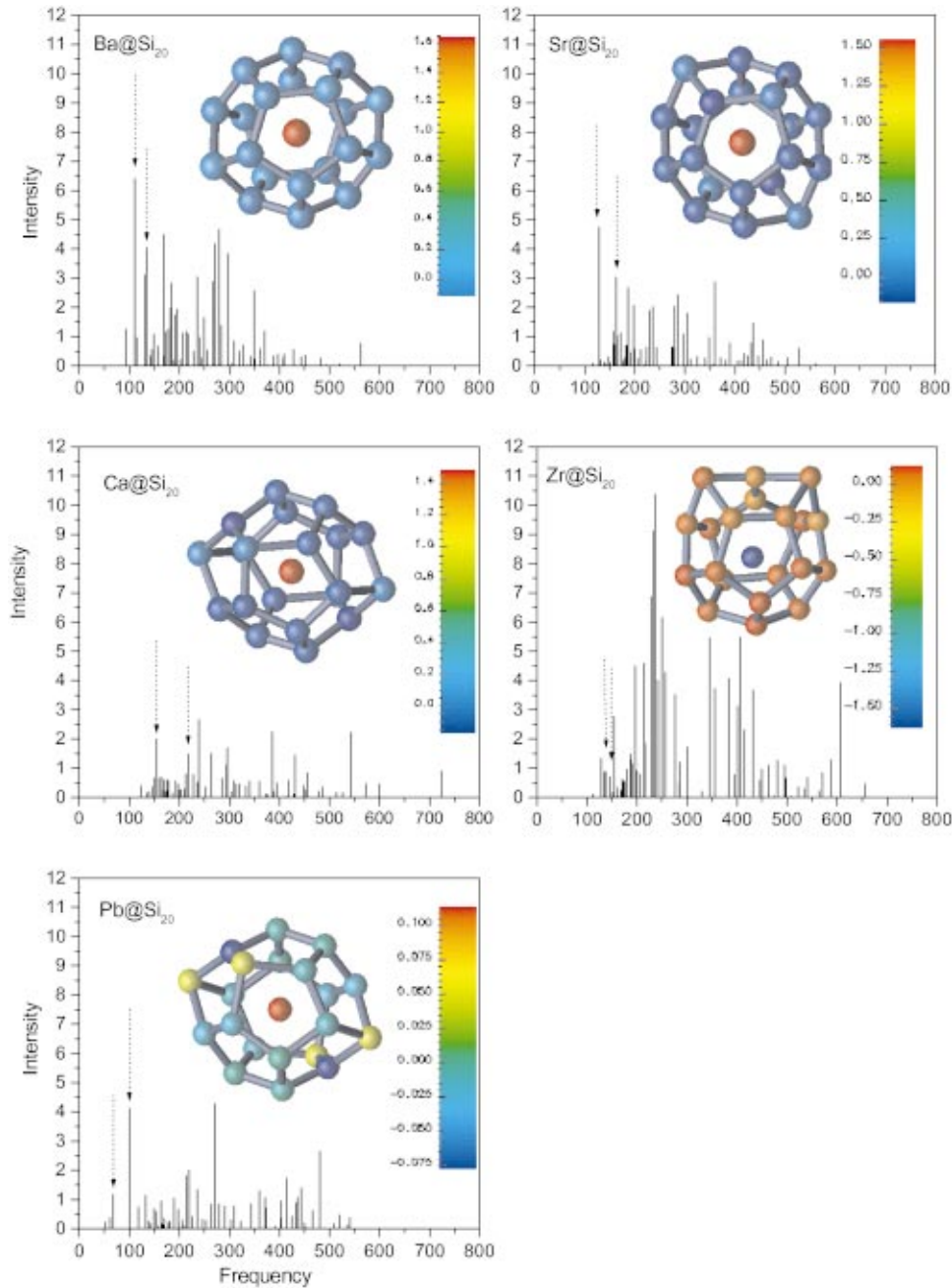


FIG. 1. (Color) Vibrational spectra and charge distributions for  $M@Si_{20}$ ,  $M = Ba, Sr, Ca, Zr,$  and  $Pb$ . The frequency is in  $cm^{-1}$ , and the IR intensity in  $km/mol$ . The color map (inset) shows the charge distribution scale for the clusters. The arrows indicate frequencies arising from the metal atom.

insulating  $C_{60}$ ,<sup>23</sup> we placed 20 Si atoms around  $C_{20}$ , but the resulting Si cage is unstable. (2) Using the icosahedral  $Al_{12}Si$  cluster, which is a well-known geometrically and electronically stable magic cluster, and considering the dual relationship between the dodecahedron and icosahedron, we placed 20 silicon atoms on the 20 faces of  $Al_{12}Si$ . However, optimizations did not lead to a stable Si cage. (3) Using 20 H atoms to terminate the dangling Si bonds, we found that the  $Si_{20}H_{20}$  cage is intrinsically unstable. (4) Finally, inspired by the Si clathrates and metal-encapsulated cage clusters of silicon, we found that Ba, Sr, Ca, Zr, and Pb atoms can stabilize the cage with a distorted dodecahedral structure.

Figure 1 shows the optimized structures together with the vibrational frequency spectra, where the colors of the atoms indicate the charge distributions, their values being shown on

the color maps, and the arrows on the frequency spectra specify the vibrational modes with large contributions from the metal atoms. We can see that the charge distributions in the cage can be tuned by changing the metal atom. Furthermore, the heavier the metal atom, the lower the corresponding frequency. For all the doped cages, all frequencies are real, verifying the dynamical stability.

In Table I we show the structural data, highest-occupied–lowest-unoccupied molecular orbital (HOMO-LUMO) gap, embedding energy, and charge on the metal atom obtained from natural bond orbital analysis.<sup>24</sup> For comparison, the sum of the atomic radii<sup>25</sup> for Si and each metal atom is also given, and this fits the cage size quite well in the cases of Ba, Sr, and Ca. Considering each of the studied clusters, we find that Ba doping gives the least distorted cage (labeled as con-

TABLE I. The structural data and energetics of the doped Si-caged clusters.  $r_1$  ( $r_2$ ) is the average bond length between the surface Si atoms (surface Si and the central metal atom), and  $r$  is the sum of the radii of the metal and Si atoms (Ref. 25).  $\Delta$  is the embedding energy for the metal atom in the cage, which is defined as the energy difference with respect to the empty cage and the isolated metal atom.  $\delta E$  is the energy difference between configuration I and configuration II.  $Q$  is the net charge on the metal atom. Bond lengths are given in Å and energy in eV.

Cluster	$r_1$	$r_2$	$r$	Gap	$\Delta$	$Q$	$\delta E$
Ba@Si <sub>20</sub>	2.438	3.409	3.410	0.991	-1.348	+1.650	-0.495
Sr@Si <sub>20</sub>	2.414	3.360	3.320	1.150	-1.967	+1.564	-0.437
Ca@Si <sub>20</sub>	2.401	3.331	3.150	1.321	-2.494	+1.493	-1.662
Zr@Si <sub>20</sub>	2.360	3.269	2.770	1.466	-11.314	-1.621	-7.977
Pb@Si <sub>20</sub>	2.411	3.333	2.920	1.231	-2.335	+0.115	-3.080

figuration I in Fig. 2) due to the close fit between the cage size (3.409 Å) and the sum of atomic radii (3.410 Å). Zr, with a small atomic radius, leads to a cage with large distortion, as was also found in Ref. 4. Regarding charge transfer to and from the Si cage, due to the fact that the electronegativity of Pb is just a little bit smaller than that of Si, a small amount of charge is transferred from the doped Pb atom. For Ba, Sr, and Ca, each with a large difference in electronegativity with respect to Si, approximately two electrons are donated to the cage. Finally, Zr receives about two electrons of charge because of its open 4*d* levels.

In order to understand the stabilization of the cage structure by doping and the reasons for distortion, we consider an ideal dodecahedron with  $I_h$  symmetry. For the ideal empty cage, the radius is found to be 3.26 Å. This large cavity corresponds to an interatomic distance of 2.326 Å between the Si atoms on the surface of the cluster, which is nearly the same as the interatomic distance in bulk Si [2.33 Å (Ref. 25)]. There are two ways to stabilize the structure: (1) The cage structure can be converted into smaller units (e.g., two Si<sub>10</sub> units) so that the cavity in the cluster is reduced and bonding is improved. (2) The structure can be doped with a metal atom to fill the cage cavity, the size of which should be large enough to provide effective bonding. Further, the interaction energy between the metal atom and the cage should compensate the energy loss that may arise from the change in the atomic distances of the Si atoms.

To explain why the cages are distorted, we give the electronic states in Table II. We can see that for the ideal empty Si<sub>20</sub> cage, the LUMO is four-fold degenerate and the HOMO is three-fold degenerate. Only two electrons occupy the

TABLE II. Orbital information for the ideal dodecahedral structures with  $I_h$  symmetry for the pure and doped Si<sub>20</sub> clusters. The number of electrons in each state is indicated in parentheses.

Orbital	Si <sub>20</sub>	Si <sub>20</sub> Ba	Si <sub>20</sub> Sr	Si <sub>20</sub> Ca	Si <sub>20</sub> Pb	Si <sub>20</sub> Zr
LUMO	$G_u$ (0)	$G_u$ (0)	$G_u$ (0)	$G_u$ (0)	$G_u$ (0)	$G_u$ (0)
HOMO	$T_g$ (2)	$H_g$ (8)	$T_g$ (4)	$T_g$ (4)	$T_g$ (4)	$T_g$ (6)
HOMO-1	$H_g$ (10)	$T_g$ (6)	$H_g$ (10)	$H_g$ (10)	$H_g$ (10)	$H_g$ (10)

HOMO levels, so it is possible to dope with metal atoms in order to fill these levels more completely. When Ba, Sr, Ca, Pb, and Zr are doped, the orders in the energy levels are unchanged except for the case of Ba, where the  $H_g$  HOMO-1 state and  $T_g$  states are exchanged. Except for Zr, the HOMO's for the doped cages are not fully occupied, and therefore Jahn-Teller distortions take place to lower the symmetry. For the case of Zr, however, the HOMO is fully occupied, and distortion can be explained from geometrical arguments. Due to the small size of the Zr atom, the cage has to be distorted to optimize strong bonding between the cage and the 4*d* states of the Zr atom.

In order to confirm that the dodecahedron is the lowest-energy structure, we choose the two most probable structures from the Si<sub>20</sub> isomers already studied<sup>11</sup> to investigate Ba@Si<sub>20</sub>: (1) The ground-state geometry of Si<sub>20</sub> is composed of two Si<sub>10</sub> clusters.<sup>7-11</sup> Due to its large size, Ba will not favorably bind in the center of a Si<sub>10</sub> cluster. Therefore, we consider an isomer with Ba connecting the two Si<sub>10</sub> clusters, labeled as configuration II in Fig. 2. However, after optimization, this structure lies 0.495 eV higher in energy than the Ba@Si<sub>20</sub> cage. (2) Similar to W@Si<sub>12</sub>,<sup>3</sup> the high-symmetry isomer of Si<sub>20</sub> is tube like, composed of three 6-member rings with Si atoms at the centers of the top and bottom rings. This isomer is just 0.165 eV higher in energy than the ground-state geometry.<sup>11</sup> When Ba is doped into this

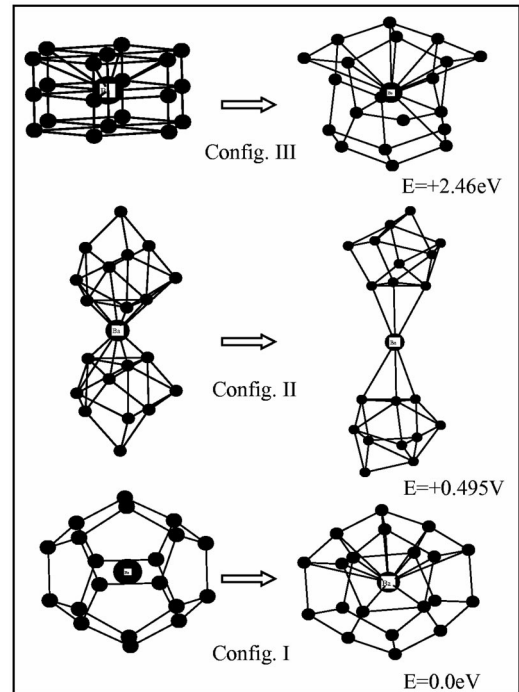


FIG. 2. Isomers of Ba@Si<sub>20</sub>. The figures on the left (right) are the initial (final relaxed) structures. Configuration I is the dodecahedral cage isomer. Configuration II is an isomer based on the ground state of Si<sub>20</sub> prolate cluster. Configuration III is based on a hexagonal prism structure of Si<sub>20</sub> that lies close in energy to the prolate structure. The relaxed structure has significant distortions and lies 2.46 eV higher in energy than configuration I (taken as zero energy). The same is also true for the other metal atoms (Sr, Ca, Zr, and Pb).

tubelike isomer (configuration III), the optimized geometry converges to a cagelike structure, composed of pentagons, squares, and hexagons, but the energy is 2.46 eV higher than the dodecahedron cage of configuration I, as shown in Fig. 2. These results show that the doped cage is energetically stable and has the lowest energy of the structures considered. Because configuration II is close in energy to configuration I, the energy differences between these two structures for the other metals are shown in the last column of Table I. We find that for the other metals, the cage structure becomes even more energetically favorable.

Finally, since Kumar and Kawazoe<sup>4</sup> found the 16 silicon atom cage to possess the closest packing for Zr encapsulation, we studied the Zr@Si<sub>20</sub> cage by capping four Si atoms on Zr@Si<sub>16</sub> in two ways: (1) symmetrical capping of the four pentagonal faces around one of the square faces and (2) placing two atoms on the neighboring pentagons around one square and two atoms opposite to these. Both of these relaxed structures lie higher in energy than configuration I, which again confirms the energetic stability of the Zr@Si<sub>20</sub> dodecahedron cage. We should also note that Jackson and Nellermoe<sup>26</sup> had shown, based on the local density approximation to density functional theory, that endohedral Zr can stabilize the Si<sub>20</sub> cluster and that this bonding is similar to endohedral bonding in small carbon fullerenes. However, in their calculations, the structure was optimized keeping the *I<sub>h</sub>* symmetry, and the intrinsic stability of the structure was not examined. The authors found that due to the d electrons in Zr, the stabilizing energy is much larger than that of an sp dopant, in agreement with our results.

The electronic states of Ba@Si<sub>20</sub> as well as the corresponding pure Si<sub>20</sub> cage are shown in Fig. 3(a). The deeper states of the silicon cage are nearly unchanged, and significant hybridization occurs between the states of the Si<sub>20</sub> cage around  $-7.5$  eV and the Ba 6s level. The states near  $-5.8$  eV, grouped near the HOMO level, do not interact significantly with Ba. However, there is a significant shift of all the states to lower energies. The hybridization with Ba leads to the occupancy of the LUMO level of the Si<sub>20</sub> cage and the opening of a larger gap. The charge density distribution of the Ba@Si<sub>20</sub> cluster is shown in Fig. 3(b), and analysis of the molecular orbitals shows that the Si atoms are bonded through *sp*-hybridized orbitals on the cage and the *s* orbitals of Ba interact with the *p* orbitals of the Si atoms.

For silicon clathrates, there are two kinds of structural units: Si<sub>20</sub>+Si<sub>24</sub> and Si<sub>20</sub>+Si<sub>28</sub>.<sup>12-16</sup> Can the Si<sub>24</sub> and Si<sub>28</sub>

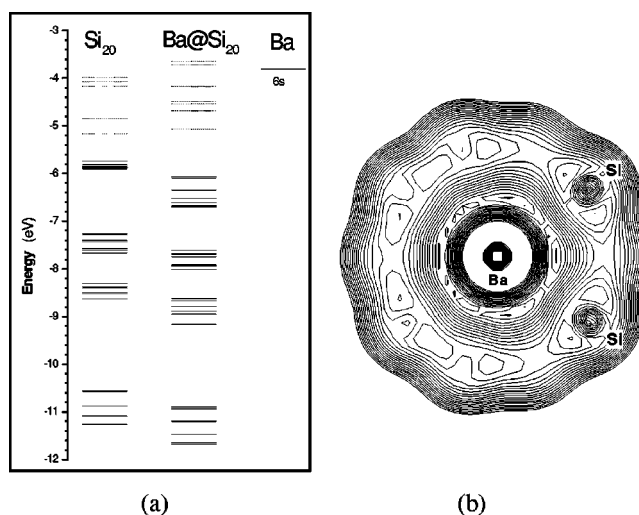


FIG. 3. (a) Eigenvalue spectra of Ba@Si<sub>20</sub> and the corresponding spectra of the Si<sub>20</sub> cage and Ba atom. The solid lines indicate the occupied states and the dotted lines the unoccupied states. (b) Total charge density distribution of Ba@Si<sub>20</sub> with contour spacing 0.005  $e/\text{\AA}^3$ .

cages also be stabilized by single atom doping? We found that due to the large size of these two cages, a single metal atom cannot stabilize; thus Si<sub>20</sub> seems to be the largest cage that can be stabilized by this kind of doping. Besides Si<sub>20</sub>, Ge<sub>20</sub> and Sn<sub>20</sub> are also the basic building blocks of Ge-based<sup>27-29</sup> and Sn-based,<sup>28</sup> clathrates respectively. Here, we also found that due to the larger size of Ge and Sn, neither Ge<sub>20</sub> nor Sn<sub>20</sub> is stabilized by doping with one metal atom, which suggests that the growth patterns of Ge and Sn are different from Si, as was also found in the case of large pure Si and Ge clusters.<sup>8</sup>

In summary, our calculations indicate that by doping with metal atoms, the dodecahedral geometry of the Si cage, which is similar to the smallest fullerene cage C<sub>20</sub>,<sup>5,6</sup> can be stabilized both dynamically and energetically. Therefore, doping is an effective way to change Si from a prolate to a caged structure that behaves like a cousin of carbon.

The authors would like to express their sincere thanks to the crew of the Center for Computational Materials Science, the Institute for Materials Research, Tohoku University, for their continuous support of the HITAC SR8000 supercomputing facility. Q.S. thanks Dr. Barbara Martinthe for kind help.

<sup>1</sup>H. W. Kroto, J. R. Heath, S. C. O'Brien, R. F. Curl, and R. E. Smalley, *Nature (London)* **318**, 162 (1985).

<sup>2</sup>S. Iijima, *Nature (London)* **354**, 56 (1991).

<sup>3</sup>H. Hiura, T. Miyazaki, and T. Kanayama, *Phys. Rev. Lett.* **86**, 1733 (2001).

<sup>4</sup>V. Kumar and Y. Kawazoe, *Phys. Rev. Lett.* **87**, 045503 (2001).

<sup>5</sup>H. Prinzbach, A. Weiler, P. Landenberger, F. Wahl, J. Wrth, L. T. Scott, M. Gelmont, D. Olevano, and B. Issendorff, *Nature (London)* **407**, 60 (2000).

<sup>6</sup>M. F. Jarrold, *Nature (London)* **407**, 26 (2000).

<sup>7</sup>K. M. Ho, A. A. Shvartsburg, B. Pan, Z. Y. Lu, C. Z. Wang, J. G. Wacker, J. L. Fye, and M. F. Jarrold, *Nature (London)* **392**, 582 (1998).

<sup>8</sup>A. A. Shvartsburg, B. Liu, Z. Lu, C. Z. Wang, M. F. Jarrold, and K. M. Ho, *Phys. Rev. Lett.* **83**, 2167 (1999).

<sup>9</sup>J. Wang, J. Zhao, F. Ding, W. Shen, H. Lee, and G.H. Wang, *Solid State Commun.* **117**, 593 (2001).

<sup>10</sup>L. Mitás, J. C. Grossman, I. Stich, and J. Tobik, *Phys. Rev. Lett.*

- 84**, 1479 (2000).
- <sup>11</sup>B. X. Li and P. L. Cao, Phys. Rev. A **62**, 023201 (2000).
- <sup>12</sup>T. Kawaguchi, K. Tanigaki, and M. Yasukawa, Phys. Rev. Lett. **85**, 3189 (2000).
- <sup>13</sup>A. San-Miguel, P. Kechelian, X. Blase, P. Mélinon, L. A. Perez, J. P. Itié, A. Polian, E. Reny, C. Cros, and M. Pouchard, Phys. Rev. Lett. **83**, 5290 (1999).
- <sup>14</sup>S. Munetoh, K. Moriguchi, K. Kamei, A. Shintani, and T. Mootooka, Phys. Rev. Lett. **86**, 4879 (2001).
- <sup>15</sup>H. Fukuoka, K. Ueno, and S. Yamanaka, J. Organomet. Chem. **611**, 543 (2000).
- <sup>16</sup>C. K. Ramachandran, P. F. McMillan, S. K. Deb, M. Somayazulu, J. Gryko, J. Dong, and O. F. Sankey, J. Phys.: Condens. Matter **12**, 4013 (2000).
- <sup>17</sup>M. J. Frisch, G. W. Trucks, H. B. Schlegel, G. E. Scuseria, M. A. Robb, J. R. Cheeseman, V. G. Zakrzewski, J. A. Montgomery, R. E. Stratmann, B. J. Burant, S. Dapprich, J. M. Millam, A. D. Daniels, K. N. Kudin, M. C. Strain, O. Farkas, J. Tomasi, V. Barone, M. Cossi, R. Cammi, B. Mennucci, C. Pomelli, C. Adamo, S. Clifford, J. Ciolowski, J. V. Ortiz, B. B. Stefanov, G. Liu, A. Liashenko, P. Piskorz, I. Komaromi, R. Gomperts, R. L. Martin, D. J. Fox, T. Keith, M. A. Alaham, C. Y. Peng, A. Nanayakkara, C. Gonzalez, M. Challacombe, P. M. W. Gill, B. G. Johnson, W. Chen, M. W. Wong, J. L. Andres, M. Head-Gordon, E. S. Replogle, and J. A. Pople, computer code GAUSSIAN, 98, Gaussian, Inc., Pittsburgh, PA, 1998.
- <sup>18</sup>A. D. Becke, J. Chem. Phys. **98**, 5648 (1993).
- <sup>19</sup>W. R. Wadt and P. J. Hay, J. Chem. Phys. **82**, 284 (1985).
- <sup>20</sup>P. J. Hay and W. R. Wadt, J. Chem. Phys. **82**, 299 (1985).
- <sup>21</sup>Q. Sun (unpublished).
- <sup>22</sup>*Handbook of Chemistry and Physics*, 74th ed., edited by D. R. Lide (CRC Press, Boca Raton, 1993).
- <sup>23</sup>X. G. Gong and Q. Q. Zheng, Phys. Rev. B **52**, 4756 (1995).
- <sup>24</sup>A. E. Reed, L. A. Curtiss, and F. Weinhold, Chem. Rev. **88**, 899 (1988).
- <sup>25</sup>C. Kittel, *Introduction to Solid State Physics* (Wiley, New York, 1976).
- <sup>26</sup>K. Jackson and B. Nellermoe, Chem. Phys. Lett. **254**, 249 (1996).
- <sup>27</sup>T. Kawaguchi, K. Tanigaki, and M. Yasukawa, Appl. Phys. Lett. **77**, 3438 (2000).
- <sup>28</sup>G. S. Nolas and C. A. Kendziora, Phys. Rev. B **62**, 7157 (2000).
- <sup>29</sup>J. F. Meng, N. V. Chandra Shekar, J. V. Badding, and G. S. Nolas, J. Appl. Phys. **89**, 1730 (2001).